Matrix Biology 132 (2024) 34–46

Contents lists available at ScienceDirect

Matrix Biology

journal homepage: www.elsevier.com/locate/matbio

MiR-214–3p regulates Piezo1, lysyl oxidases and mitochondrial function in human cardiac fibroblasts

Christopher J. Trevelyan [a], Amanda D.V. MacCannell [a], Leander Stewart [a], Theodora Tarousa [a,b], Hannah A. Taylor [a], Michael Murray [a], Sumia A. Bageghni [a], Karen E. Hemmings [a], Mark J. Drinkhill [a], Lee D. Roberts [a], Andrew J. Smith [b], Karen E. Porter [a], Karen A. Forbes [a], Neil A. Turner [a,*]

[a] Leeds Institute of Cardiovascular and Metabolic Medicine (LICAMM), School of Medicine, University of Leeds, Leeds LS2 9JT, UK
[b] School of Biomedical Sciences, Faculty of Biological Sciences, University of Leeds, Leeds LS2 9JT, UK

ARTICLE INFO

Keywords:
Cardiac fibroblast
microRNA
miR-214
Piezo1
Lysyl oxidase
Mitochondrial dysfunction

ABSTRACT

Cardiac fibroblasts are pivotal regulators of cardiac homeostasis and are essential in the repair of the heart after myocardial infarction (MI), but their function can also become dysregulated, leading to adverse cardiac remodelling involving both fibrosis and hypertrophy. MicroRNAs (miRNAs) are noncoding RNAs that target mRNAs to prevent their translation, with specific miRNAs showing differential expression and regulation in cardiovascular disease. Here, we show that miR-214–3p is enriched in the fibroblast fraction of the murine heart, and its levels are increased with cardiac remodelling associated with heart failure, or in the acute phase after experimental MI. Tandem mass tagging proteomics and in-silico network analyses were used to explore protein targets regulated by miR-214–3p in cultured human cardiac fibroblasts from multiple donors. Overexpression of miR-214–3p by miRNA mimics resulted in decreased expression and activity of the Piezo1 mechanosensitive cation channel, increased expression of the entire lysyl oxidase (LOX) family of collagen cross-linking enzymes, and decreased expression of an array of mitochondrial proteins, including mitofusin-2 (MFN2), resulting in mitochondrial dysfunction, as measured by citrate synthase and Seahorse mitochondrial respiration assays. Collectively, our data suggest that miR-214–3p is an important regulator of cardiac fibroblast phenotypes and functions key to cardiac remodelling, and that this miRNA represents a potential therapeutic target in cardiovascular disease.

Introduction

Advances in current understanding of cardiac fibroblast (CF)[1] function have highlighted the imperative role this cell type plays in cardiac homeostasis and cardiovascular disease. CF are crucial for cardiac development and physiology, as well as wound healing and repair, and are also key drivers of adverse pathological cardiac remodelling [1]. CF undergo a phenotypic switch to a myofibroblast (MyoFb) phenotype during cardiac remodelling which is typified by increased proliferation and dysregulation of extracellular matrix (ECM) protein production, leading to rapid ECM turnover, fibrosis and subsequent thickening of the myocardium, with diminished cardiac contractility [2]. Epigenetic mechanisms are thought to contribute to the persistence of the MyoFb phenotype [3], for example in CF cultured from diabetic patients that maintain an inherent profibrotic phenotype in culture [4]. One such form of epigenetic regulation that can regulate CF function is the activity of microRNAs (miRNAs).

MiRNAs are short, non-coding RNAs around 22 nucleotides in length

* Corresponding author: Discovery and Translational Science Department, Leeds Institute of Cardiovascular and Metabolic Medicine (LICAMM), LIGHT Laboratories, Clarendon Way, University of Leeds, Leeds LS2 9JT, UK.
E-mail address: n.a.turner@leeds.ac.uk (N.A. Turner).

[1] CF, cardiac fibroblast; CS, citrate synthase; CTGF, connective tissue growth factor; ECM, extracellular matrix; FCS, foetal calf serum; FDR, false discovery rate; FGM, full growth medium; IPA, Ingenuity Pathway Analysis software; ISO, isoproterenol; LOX, lysyl oxidase; LOXL, LOX-like; MFN2, mitofusin-2; MI, myocardial infarction; miRNA, microRNA; MMP, matrix metalloproteinase; MyoFb, myofibroblast; NC, negative control; SBS, standard bath solution; SFM, serum-free medium; STRING, Search Tool for the Retrieval of Interacting Genes/Proteins software; TMT, tandem mass tagging; UTR, untranslated region.

https://doi.org/10.1016/j.matbio.2024.06.005
Received 18 January 2024; Received in revised form 20 May 2024; Accepted 20 June 2024
Available online 25 June 2024

which function by binding to complementary seed sequences in the 3′ untranslated region (UTR) of messenger RNA (mRNA) molecules to target their degradation or block the binding of ribosomes, with the net result being inhibition of protein synthesis [5]. The main canonical pathway for miRNA biogenesis involves transcription of primary miRNAs (pri-miRs), which contain a characteristic hairpin as part of their structure which forms a pri-miR duplex [6]. Upon recognition and binding by the DiGeorge Syndrome Critical Region 8 (DGCR8) protein, the enzyme Drosha catalyses the cleavage of the hairpin which ultimately results in generation of a pre-miR. Subsequent processing occurs in the cytoplasm and transport from the nucleus is facilitated by an exportin 5 (XPO5)/RanGTP complex. The pre-miR is processed to remove the terminal loop which produces a mature miRNA duplex, and this step is catalysed by the RNase III endonuclease, Dicer. A key result of this processing is the directionality of the miRNA strand that is produced, depending on whether the strand arises from the 5′ end or 3′ end of the pre-miRNA hairpin, with these strands referred to as 5p and 3p respectively. The biologically active guide strand of miR-214 is miR-214–3p [7], and this is the strand that we have investigated in the present study.

Specific miRNAs are dysregulated in both the main phenotypes of cardiac remodelling, namely fibrosis and hypertrophy. Perhaps the best known in this context is miR-21, which is regarded as a CF-enriched profibrotic miRNA that functions to increase CF proliferation, differentiation and ECM turnover through its regulation of downstream target mRNAs [8]. For example, it has been demonstrated that miR-21 promotes CF-to-MyoFb transformation via its targeting of *Jagged1* in mice and that removal of miR-21 activity by sponging in a murine myocardial infarction (MI) model protected against myocardial fibrosis [9]. Previous work from our group found that the expression of a small number of specific miRNAs (including miR-21 and miR-214–3p) were increased in an isoproterenol-induced (ISO) model of heart failure in mice, with this increase being dependent upon fibroblast-specific expression of the stress activated MAP kinase, p38α [10].

In contrast to miR-21, there is no clear consensus regarding the actions of miR-214–3p and whether its activity induces a profibrotic or antifibrotic phenotype. For example, miR-214–3p has been reported to be a repressor of CF-to-MyoFb transformation and of CF proliferation through targeting the *Nlrc5* pattern recognition receptor gene [11], whereas others have reported that miR-214–3p induces rat CF proliferation via inhibition of the mitochondrial fusion gene, *Mitofusin 2* (*Mfn2*) [12]. The diverse roles of miR-214–3p, and conflicting evidence regarding its role in fibroblast proliferation, activation and collagen synthesis, as well as pathological hypertrophy and fibrosis, have recently been reviewed [13]. This lack of consensus is not limited to cardiovascular disease, as miR-214–3p has been shown to inhibit

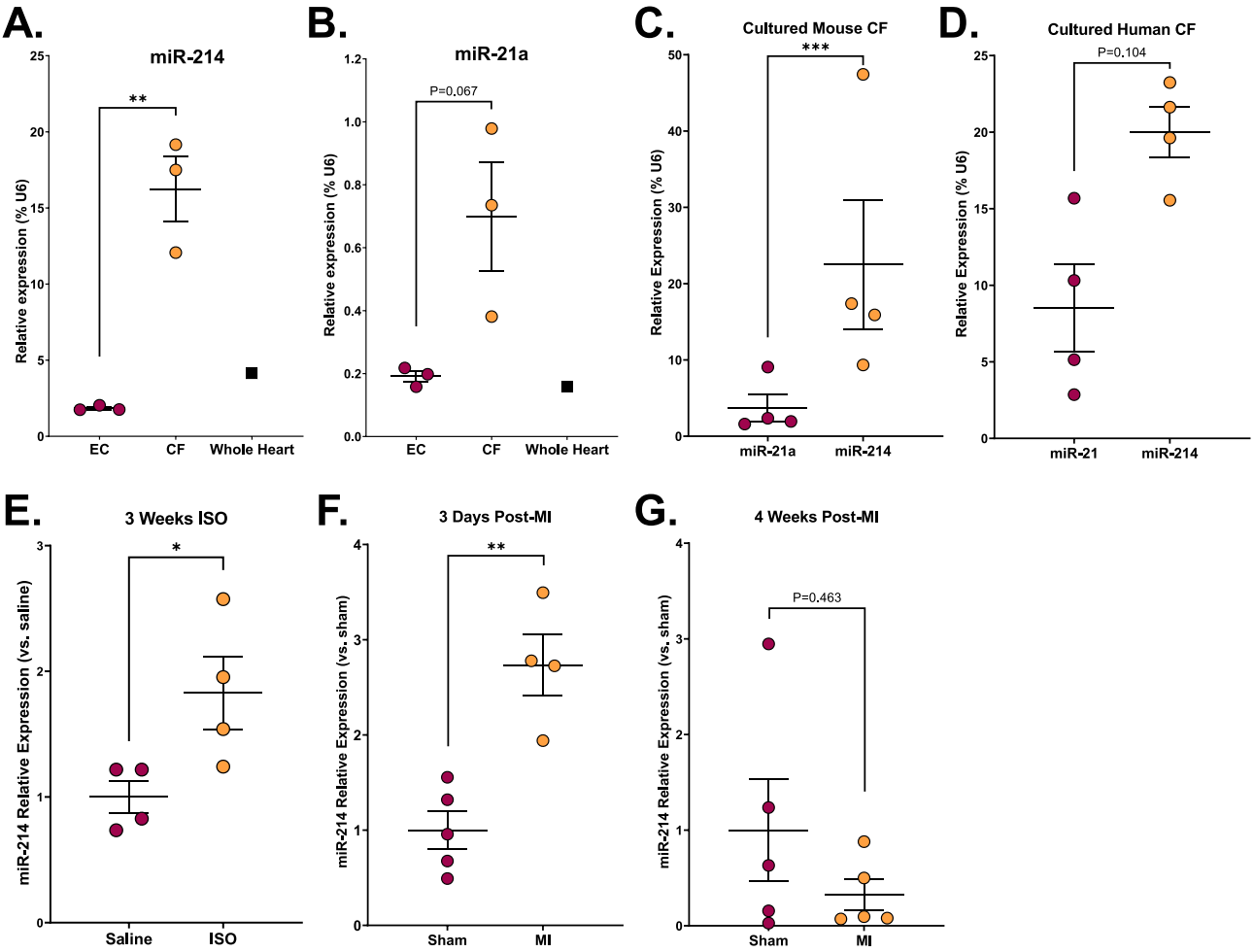

Fig. 1. Analysis of miR-214–3p expression in murine and human cardiac fibroblasts and in the remodelling murine heart. (A, B) MiR-214–3p (A) and miR-21 (B) expression levels in mouse heart cell fractions comprising endothelial cells (EC; $n = 3$), cardiac fibroblasts (CF; $n = 3$) or all cell types present in a representative whole heart ($n = 1$). All data normalized to U6 housekeeper. (C, D) MiR-21 and miR-214–3p expression in cultured mouse CF (C) and human CF (D) ($n = 4$ per group). (E) Cardiac (whole heart) miR-214–3p expression in a murine model of heart failure involving 3 weeks isoproterenol (ISO) infusion compared to saline control ($n = 4$ per group). (F, G) Cardiac (whole heart) miR-214–3p expression in a murine model of myocardial infarction (MI) compared to sham control after 3 days (F) or 4 weeks (G) ($n = 4$–5 per group). ***$P < 0.001$; **$P < 0.01$, *$P < 0.05$.

proliferation and invasion in human hepatocellular carcinoma (HCC) through the targeting of beta catenin (*CTNNB1*) [14], whereas miR-214–3p promotes cell proliferation in ovarian cancer through the targeting of phosphatase and tensin homolog (*PTEN*) [15].

In the present study we investigated the expression of miR-214–3p in isolated and cultured CF and in mouse models of cardiovascular disease, before evaluating its role in human CF proliferation. We then employed tandem mass tagging (TMT) proteomics to investigate the effect of miR-214–3p overexpression on the human CF proteome and conducted in-silico network analyses to predict potential functional consequences of miR-214–3p overexpression, with follow-up functional experiments.

Results

MiR-214–3p is enriched in cardiac fibroblasts and its levels are increased with cardiac remodelling

We firstly determined which cardiac cell types express miR-214–3p by analysing isolated cell fractions from mouse hearts (Fig. 1A). MiR-214–3p expression was 8.8-fold higher in fibroblast fractions compared to endothelial cells, and 3.9-fold higher than whole heart, which contained all cell types including cardiomyocytes. This suggests a strong enrichment of miR-214–3p in fibroblasts. As a positive control, a comparable pattern was observed for miR-21, a well-known CF-enriched miRNA, with 3.6-fold higher expression in CF compared to endothelial cells, and 4.4-fold enrichment compared with whole heart (Fig. 1B).

Next, we measured expression of miR-214–3p in cultured CF to see if this enrichment was also evident in cell culture. MiR-214–3p was highly expressed at levels 6.0-fold and 2.4-fold higher than miR-21 in cultured mouse CF (Fig. 1C) and human CF (Fig. 1D) respectively.

Subsequently, the expression levels of miR-214–3p were measured in mouse heart samples representing different types and stages of cardiac remodelling: 3 weeks post-ISO treatment (heart failure model), and 3 days and 4 weeks post- left anterior descending artery (LAD) ligation (MI model; inflammatory and reparative phases respectively). Cardiac (i.e. whole heart) miR-214–3p levels were elevated by 83 % in hearts from ISO-treated mice compared to saline control (Fig. 1E). Furthermore, miR-214–3p levels were elevated by 2.7-fold at 3 days post-LAD ligation compared to sham (Fig. 1F), but showed no significant difference after 4 weeks (Fig. 1G).

Having confirmed high expression and enrichment of miR-214–3p in CF, and its upregulation during cardiac remodelling, we proceeded to investigate the functional effect of miR-214–3p on human CF proliferation following miR-214–3p overexpression.

Effect of miR-214–3p overexpression on human cardiac fibroblast proliferation

Firstly, we confirmed that transfection with small, chemically modified double-stranded RNA molecules designed to mimic endogenous mature miR-214–3p ("pre-miR-214–3p") resulted in significantly higher levels of miR-214–3p, compared to transfection with pre-miR negative control ("pre-miR-NC") (Fig. 2A). We also confirmed that pre-miR-214–3p transfection did not result in altered levels of other miRNAs that we had previously identified as altered in our ISO infusion model of heart failure [10], namely miR-21, miR-224 and miR-30d (Fig. 2A).

The role of miR-214–3p in regulating human CF cell proliferation was investigated by transfecting with pre-miR-214–3p and measuring the effect on cell number over a 7-day period in either serum-free medium (SFM) (Fig. 2B) or medium containing 2.5 % foetal calf serum (FCS) (Fig. 2C). No difference was observed between pre-miR-214–3p transfected cells and cells transfected with pre-miR-NC, suggesting that miR-214–3p does not regulate human CF proliferation under these conditions.

After observing no effect on CF proliferation, we next conducted experiments to measure the effect of increased miR-214–3p expression on the entire human CF proteome.

Effect of miR-214–3p overexpression on the human cardiac fibroblast proteome

To understand the influence of miR-214–3p on the CF proteome, protein lysates from cultured human CF derived from 6 donors were analysed using TMT proteomics 72 h after pre-miR-214–3p or pre-miR-NC transfection (Fig. 3A). 8793 proteins were initially identified and, after excluding non-human proteins, contaminants and proteins that fell below the false discovery rate (FDR) cut-off, it was revealed that 3366

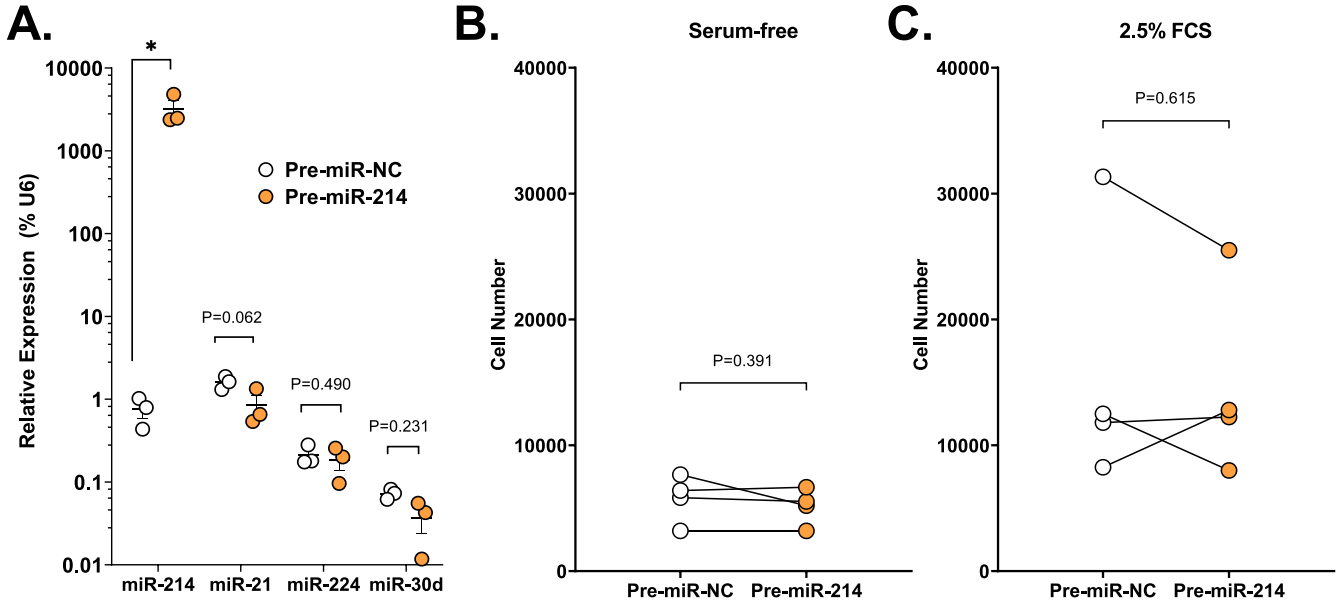

Fig. 2. Effect of miR-214–3p overexpression on human cardiac fibroblast proliferation. (A) Expression levels of miR-214–3p, −21, −224 and −30d measured 48 h after transfection of human CF with pre-miR negative control (NC; open symbols) or pre-miR-214–3p (coloured symbols). *$P < 0.05$, ns=not significant ($n = 3$). Note log scale. (B, C) Proliferation of human CF following transfection with pre-miR NC or pre-miR-214–3p over a 7-day period in SFM (B) or 2.5 % FCS-containing medium (C). Paired data from different donor cell populations are linked. ns=not significant ($n = 4$).

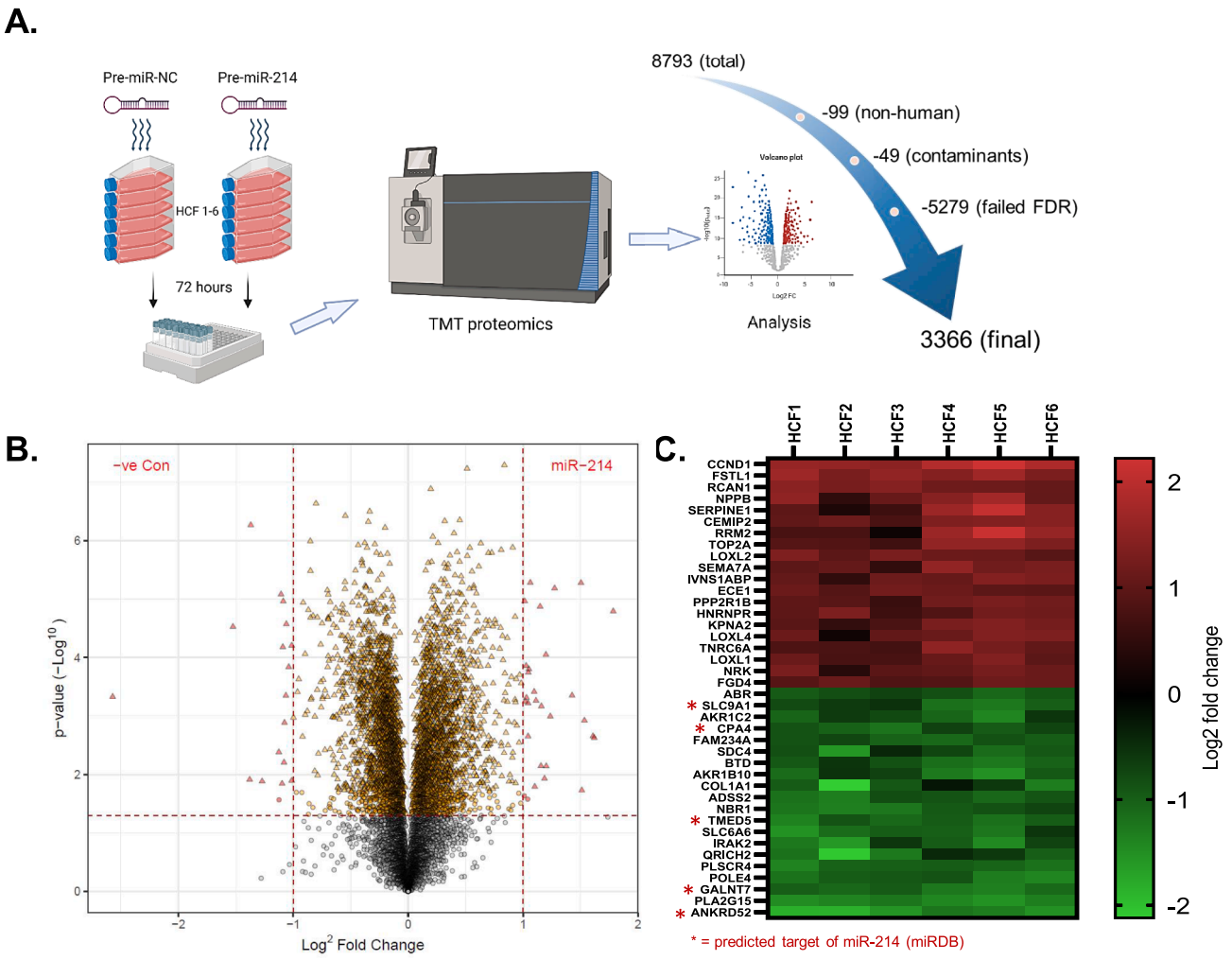

Fig. 3. Effect of miR-214–3p over-expression on the human cardiac fibroblast proteome. (A) Schematic diagram of workflow for TMT proteomics analysis performed on human CF from 6 donors 72 h after transfection with pre-miR-NC or pre-miR-214–3p. Of the 8793 total proteins identified, 3366 were significantly altered by miR-214–3p overexpression and analysed further. (B) Volcano plot showing log2 fold change in expression of 8793 individual proteins (x axis) versus P value (y axis) following miR-214–3p overexpression. Circles = fell below 5 % cut-off for FDR (false discovery rate), triangles = passed FDR. (C) Heat map of individual log2 fold changes for each patient sample (HCF1–6) for the 20 most increased (top, red) and 20 most decreased (bottom, green) proteins. Asterisks identify proteins that are predicted / known miR-214–3p targets according to the miRDB.org database.

proteins were differentially expressed following miR-214–3p over-expression (Fig. 3B). The 20 proteins with most increased expression and the 20 with most decreased expression were plotted on a heatmap to visualize the reproducibility between donor cell populations; confirming consistency between samples (Fig. 3C). Furthermore, in-silico analysis using the miRDB.org database revealed that 5 of the 20 most down-regulated proteins observed were predicted targets of miR-214–3p; namely ANKRD52, GALNT7, TMED5, CPA4 and SLC9A1 (depicted by asterisks in Fig. 3C). Conversely, and as expected, none of the top 20 most increased proteins appeared in the miR-214–3p target database.

The proteomics data also enabled confirmation of the identity of the cell populations cultured from the donor heart samples as being fibroblasts. All cultures expressed high levels of the fibroblast markers vimentin, S100A4 (FSP1), PDGFRA, DDR2, THY1 (CD90), COL1A1 and COL3A1, along with the myofibroblast marker αSMA (ACTA2) (Table 1). Importantly, cultures showed a complete absence of cardiomyocyte marker MYH6, endothelial cell marker PECAM1 and smooth muscle cell marker MYH11 (Table 1). These data confirm the CF cultures used for analysis of miR-214–3p function were free of contamination from other cardiac cell types.

These investigations also revealed that pre-miR-214–3p over-expression led to significant increases in protein expression of CF cell surface markers DDR2 (33 % increase) and THY1 (43 % increase), and reductions in protein expression of COL1A1 (34 % reduction) and COL3A1 (29 % reduction) (Table 1). A follow-up experiment confirmed that the miR-214–3p-driven reduction in COL1A1 protein was also evident at the mRNA level, with a 36 % reduction measured 48 h after transfection, indicating that the repressive effects of miR-214–3p on type I collagen protein expression were likely due to reduced *COL1A1* mRNA levels (Fig. 4). Analysis of additional collagen subtypes expressed by CF is summarised in **Supplemental Table 1**. In addition to abundant levels of collagen I (COL1A1/COL1A2) and collagen III (COL3A1), lower abundances of collagens IV (COL4A1/COL4A4), V (COL5A1), VI (COL6A3) and XIV (COL14A1) were observed, in agreement with the known collagen expression profile for CF [16]. Some of these other collagens were also modulated by miR-214–3p over-expression, albeit to a lesser extent than collagens I and III. Although most were reduced in response to miR-214–3p overexpression, collagen V levels were increased (**Supplemental Table 1**).

MiR-214–3p overexpression reduces Piezo1 mechanosensitive ion channel expression and activity in human cardiac fibroblasts

We recently described the expression, signalling and function of the

Table 1
Proteomics analysis of cell-type markers in human cardiac fibroblast cultures. Well-established markers of cardiac cell-types were examined in the control TMT proteomics dataset and their mean normalized abundance calculated. Effects of pre-miR-214–3p transfection were evaluated and expressed as Log2 fold change (FC) with P value from bioinformatics analysis of human CF from six donors.

Cell-type	Marker Protein	Mean Normalised Abundance	Pre-miR-214 Log^2FC	Statistical significance
Cardiomyocytes	αMHC (MYH6)	Undetectable	–	–
Endothelial cells	PECAM1 (CD31)	Undetectable	–	–
Smooth muscle cells	SM-MHC (MYH11)	Undetectable	–	–
Smooth muscle cells & myofibroblasts	αSMA (ACTA2)	89.9	No change	ns
Fibroblasts	Vimentin	17,988.6	No change	ns
	S100A4 (FSP1)	3188.5	No change	ns
	PDGFRA	2387.4	No change	ns
	DDR2	1122.7	0.41	$P = 0.0003$
	THY1 (CD90)	418.8	0.52	$P = 0.0016$
	COL1A1	15,840.9	−0.60	$P = 0.0011$
	COL3A1	8599.6	−0.49	$P = 0.0003$

novel mechanosensitive cation channel Piezo1 in human and mouse CF, with implications for cardiac remodelling [17,18]. We therefore adopted a candidate protein approach and interrogated our TMT dataset to determine whether miR-214–3p was able to modulate Piezo1 protein levels in human CF. MiR-214–3p overexpression decreased Piezo1 protein expression by 38 % (Fig. 5A), with Piezo1 being ranked as the 55th most downregulated protein (out of a total of 1798 downregulated proteins) in the entire dataset. It was further established by RT-PCR that miR-214–3p overexpression decreased *PIEZO1* mRNA expression by 40 % after 48 h (Fig. 5B), suggesting that the inhibitory effect of miR-214–3p on Piezo1 protein expression was due to reduced *PIEZO1* mRNA levels. Indeed, exploration of the 3′UTR of PIEZO1 mRNA using the miRNA binding target prediction tool TargetScan revealed a 7-nucleotide consensus binding sequence for miR-214–3p (CCTGCTG) (**Supplemental Fig. 1**). To confirm whether miR-214–3p-mediated downregulation of Piezo1 affected Ca^{2+} signalling at a functional level, a Fura-2-based ratiometric assay was performed using the specific Piezo1 agonist Yoda1 [19] (Fig. 5C, D). Yoda1-induced Ca^{2+} influx was reduced by 60 % 72 h after pre-miR-214–3p transfection compared with pre-miR-NC control. This was not a generic effect on Ca^{2+} signalling, as the Ca^{2+} influx in response to ATP remained unaffected by pre--miR-214–3p transfection (Fig. 5C, D).

Lysyl oxidase (LOX) family proteins are upregulated by miR-214–3p in human CF

We next employed unbiased network analysis approaches to explore the targets of miR-214–3p. Functional enrichment analysis using Search Tool for the Retrieval of Interacting Genes/Proteins (STRING) revealed that the most significant network associated with the 50 most reproducibly altered proteins (ranked by P value, irrespective of direction of change; Fig. 6A), was "acetylation". No functional networks were identified for the 50 most downregulated proteins (data not shown), however analysis of the 50 most increased proteins yielded the largest number of linked protein networks, with the most enriched pathways being "ECM organization", "protein-lysine 6-oxidase activity" and "peptidyl lysine oxidation" (Fig. 6B). Lysyl oxidase (LOX) family proteins were central to all these networks. Indeed, miR-214–3p overexpression promoted up-regulation of the entire family of LOX proteins (LOX, LOXL-1, LOXL-2, LOXL-3 and LOXL-4), with a fold-change of between 1.3 and 2.2 for each compared to pre-miR-NC transfection (Fig. 6C). A 1.5- to 2.0-fold increase in mRNA levels of each LOX family member was also observed in response to pre-miR-214–3p in a separate cohort of human CF samples collected 48 h after transfection (Fig. 6D). STRING analysis revealed that LOX family members shared networks with one another, along with connective tissue growth factor (CTGF) and matrix metalloproteinase-1 (MMP1) (Fig. 6B), two additional ECM-regulating proteins that were upregulated by miR-214–3p overexpression by 89 % and 79 % respectively in the TMT proteomics screen.

To investigate if there was any interplay between Piezo1 activity (decreased by pre-miR-214–3p) and LOX family protein expression (increased by pre-miR-214–3p), we treated human CF with the Piezo1 activator, Yoda1 for 6–24 h before measuring LOX family mRNA

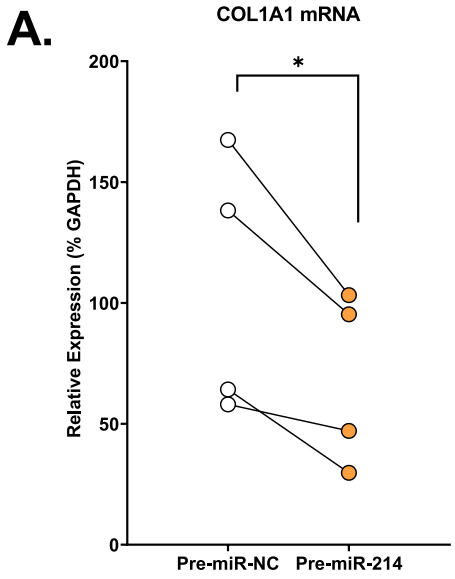

B.

COL1A1	Protein (TMT)	mRNA (qRT-PCR)
Time (n)	72 h (n=6)	48 h (n=4)
Pre-miR-214 Fold Change	0.66	0.64
P Value	0.0011	0.0302

Fig. 4. MiR-214–3p over-expression reduces type I collagen expression at protein and mRNA levels in human cardiac fibroblasts. (A) mRNA expression levels of COL1A1 gene measured 48 h after transfection of human CF with pre-miR negative control (NC) or pre-miR-214–3p. Paired data from different donor cell populations are linked. *$P < 0.05$ ($n = 4$). (B) Summary of protein and mRNA fold-change data for COL1A1 protein/gene.

A.

PIEZO1	Protein (TMT)	mRNA (qRT-PCR)
Time (n)	72 h (n=6)	48 h (n=7)
Pre-miR-214 Fold Change	0.62	0.60
P Value	$3.86x10^{-5}$	0.0032

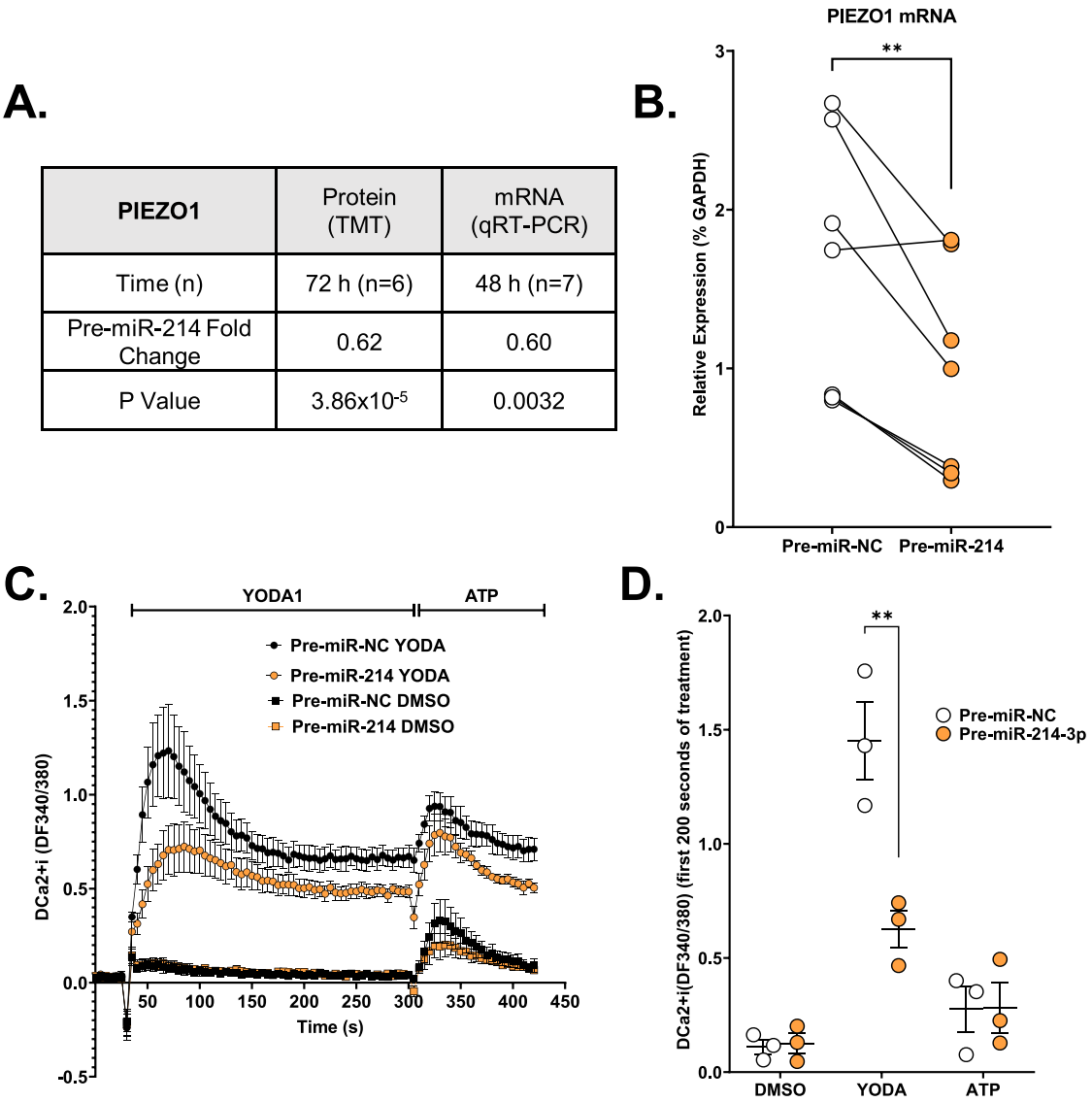

Fig. 5. MiR-214–3p overexpression reduces Piezo1 mechanosensitive cation channel expression and activity in human cardiac fibroblasts. (A) Summary of protein and mRNA fold-change data for PIEZO1 protein/gene. (B) PIEZO1 mRNA expression levels measured 48 h after transfection of human CF with pre-miR negative control (NC) or pre-miR-214–3p. Paired data from different donor cell populations are linked. $^{**}P < 0.01$ ($n = 7$). (C) Representative Ca^{2+} traces obtained from human CF 72 h after transfection with pre-miR NC or pre-miR-214–3p. Stimuli were added after 30 s; Piezo1 activator, Yoda 1 (5 μM) or DMSO vehicle, followed by ATP (5 μM) after 300 s. (D) Summary data of peak amplitudes in response to DMSO, Yoda1 or ATP in transfected cells from different donors. $^{**}P < 0.01$ ($n = 3$).

expression levels (**Supplemental Fig. 2**). Yoda1 treatment for 24 h reduced *LOX, LOXL1* and *LOXL4* mRNA expression by 52 %, 55 % and 67 % respectively, suggesting that Piezo1 activity negatively regulates LOX family expression.

Mitochondrial protein networks and mitochondrial function are reduced by miR-214–3p in human cardiac fibroblasts

Parallel analysis of protein networks using Ingenuity Pathway Analysis (IPA) revealed that proteins altered by miR-214–3p overexpression were involved in pathways associated with mitochondrial dysfunction. The two most affected pathways following miR-214–3p overexpression were identified as “mitochondrial dysfunction” and “oxidative phosphorylation” (with -log P values of 32.8 and 26.2 respectively) (Fig. 7A). Further investigation revealed that the majority of mitochondrial proteins across each complex of the electron transport chain were downregulated by miR-214–3p, as depicted in the “oxidative phosphorylation” (Fig. 7B) and “mitochondrial dysfunction” (**Supplemental Fig. 3**) pathway schematics. The pre-miR-214–3p-induced fold-change of some of the component proteins of Complex I (NADH:ubiquinone oxidoreductase; NDUFs) and Complex II (succinate dehydrogenases; SDHs) are tabulated, along with the miR-214–3p:mRNA targeting prediction scores from a range of target databases (Fig. 7C), confirming that at least some of these (especially NDUFC2 and MFN2) are known or predicted miR-214–3p targets.

To experimentally validate the IPA functional enrichment analysis predictions, the effect of miR-214–3p overexpression on mitochondrial function was assessed experimentally in human CF transfected with pre-miR-214–3p. There was a 58 % reduction in citrate synthase (CS) activity, a marker of mitochondrial density and TCA cycle flux [20], in pre-miR-214–3p-transfected cells compared to those transfected with pre-miR-NC (Fig. 7D), thus confirming that miR-214–3p causes a reduction in mitochondrial density. To further validate the functional prediction, mitochondrial respiration was measured in human CF transfected with pre-miR-NC or pre-miR-214–3p by performing a Seahorse Assay (Fig. 7E). Pre-miR-214–3p transfection led to a significant decrease in basal respiration, oxidative phosphorylation coupled respiration and maximal uncoupled respiration, indicating impaired

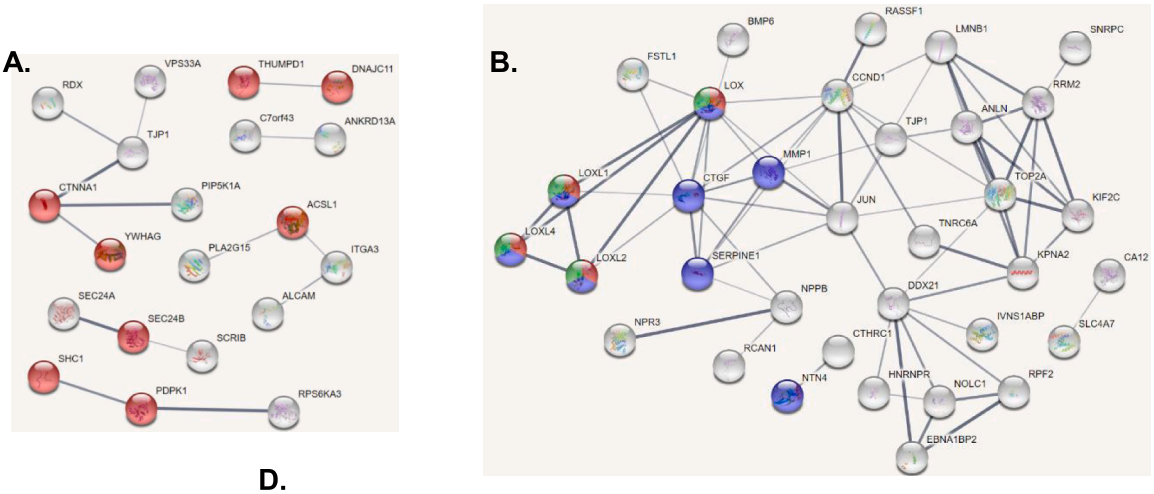

	Pre-miR-214 Fold Change	
Family member	Protein 72 h (n=6)	mRNA 48 h (n=3)
LOX	1.74	1.65
LOXL1	2.04	1.71
LOXL2	2.22	1.67
LOXL3	1.39	1.51
LOXL4	2.06	1.97

Fig. 6. Lysyl oxidase (LOX) family proteins are up-regulated by miR-214–3p in human cardiac fibroblasts. (A) STRING protein network analysis of the 50 most reproducibly altered proteins (ranked by P value, irrespective of direction of change). The most enriched pathway was "acetylation" (red). (B) STRING protein network analysis of the 50 most increased proteins (ranked by fold-change). The most enriched pathways were "ECM organization" (blue), "protein-lysine 6-oxidase activity" (green) and "peptidyl lysine oxidation" (red). (C) Summary of protein and mRNA fold-change data for LOX family proteins/genes. (D) mRNA expression levels of LOX family genes measured 48 h after transfection of human CF with pre-miR negative control (NC) or pre-miR-214–3p. Paired data from different donor cell populations are linked. $^{**}P < 0.01$, $^{*}P < 0.05$ ($n = 3$).

mitochondrial function.

Down-regulation of mitochondrial fusion proteins can reduce mitochondrial efficiency leading to mitochondrial dysfunction. It was noteworthy that the mitochondrial fusion protein MFN2, which was reduced by 25 % in the proteomics screen, was ranked by miRDB as the 11th strongest target of miR-214–3p (it was also a predicted target in all databases examined) (Fig. 7C). Analysis of the 3′UTR sequence of the human *MFN2* mRNA revealed the presence of three distinct 6/7-nucleotide sequences for which miR-214–3p shares complementarity and could potentially target and recognize as a miRNA seed sequence (**Supplemental Fig. 4**). RT-PCR confirmed that miR-214–3p overexpression resulted in a 43 % decrease in *MFN2* mRNA levels 48 h post-transfection (Fig. 7F), suggesting that direct reduction of *MFN2* mRNA underlies the effect on MFN2 protein. Western blotting analysis confirmed the reduction in MFN2 protein originally identified in the TMT proteomics screen (Fig. 7G). No interplay between Piezo1 activity and MFN2 mRNA expression was observed in studies with Yoda 1 (**Supplemental Fig. 2**).

Discussion

MiR-214–3p is emerging as a key regulator of (patho)physiology in cardiovascular disease, cancer, bone formation and cell differentiation [13]. In the present study, we focused on its regulation in the remodelling mouse heart and more specifically in modulating protein networks regulating fibroblast function using cultured human CF. Our data have uncovered new regulatory targets and networks that may offer promising therapeutic avenues for treating cardiac pathologies.

Our murine studies revealed elevated cardiac expression of miR-214–3p in a heart failure model (3 weeks ISO infusion) and in the acute inflammatory phase of post-MI remodelling (3 days after LAD ligation), but not in the chronic reparative post-MI phase (4 weeks after LAD ligation). Expression of miR-214–3p has previously been shown to be elevated in the heart 7 days after ischemia/reperfusion injury [21], 7 days post-ISO infusion [12] and at 2 weeks post-Ang II infusion [22]. This could mean that although ISO infusion and LAD ligation lead to differing cellular responses, the important factor in miR-214–3p activity in response to any of these mediators of cardiac remodelling is the time point and phase of remodelling. Adverse, dysregulated remodelling is typically identified at the late stage following events such as MI whereas the acute phase is generally regarded as essential and typified by wound repair [23]. Therefore, miR-214–3p may play an essential and protective role in cardiac remodelling, where its activity regulates proteins that produce a phenotype of activated CF, only at the time point where their activity is needed. Indeed, global genetic deletion of miR-214–3p in mice exacerbates adverse cardiac remodelling and worsens cardiac function after ischemia/reperfusion injury [21]. From a clinical translational perspective, this suggests that miR-214–3p overexpression in the early inflammatory phase of cardiac remodelling post-MI may play a protective role and therapies aimed at increases miR-214–3p levels might be beneficial.

One of the hallmarks of cardiac remodelling is increased proliferation of CF and previous reports have either suggested proliferation is enhanced [12] or repressed [11] by the activity of miR-214–3p. Although this proliferation is necessary at the early stages of remodelling, it can become dysregulated at the latter stages, especially seen when CF differentiate into MyoFb [24]. Our finding, that the overexpression of miR-214–3p has no effect on CF proliferation rates, contrasts with these prior reports [11,12]. A notable difference between our investigation, using adult human CF, and these former reports is that they used neonatal rat or mouse CF and so the miR-214–3p-mediated

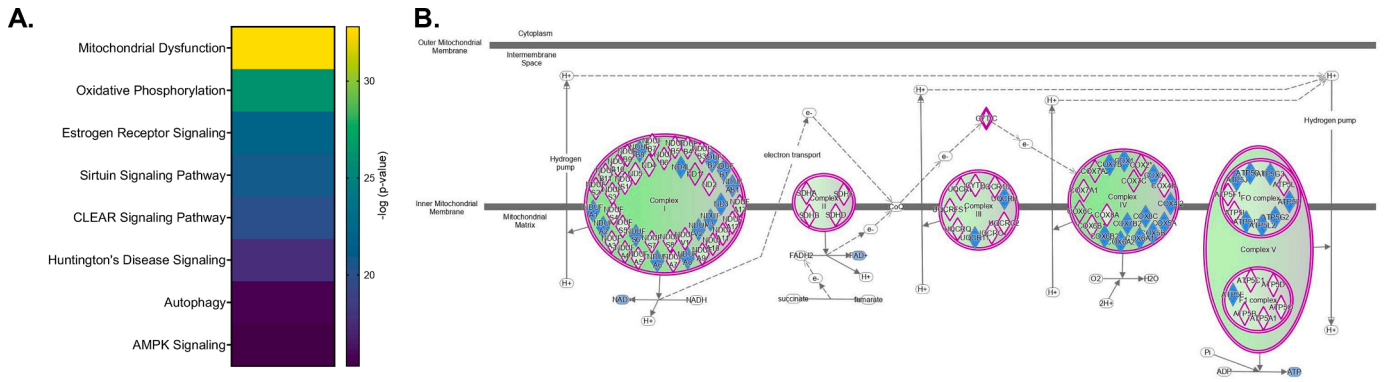

C.

Protein	Pre-miR-214 FC	miRabel score (rank)	PITA	miRanda	SVMicrO	TargetScan	miRDB score (rank)
MFN2	0.75	0.01716 (948)	1226	2144	3630	2423	97 (11)
NDUFAF4	0.77	-	-	-	-	-	-
NDUFC2	0.78	0.00385 (239)	874	461	4145	75	61 (646)
NDUFA4	0.79	0.99296 (10,410)	-	-	11366	4971	-
SDHA	0.88	0.99409 (10,675)	-	-	13606	5402	-
SDHC	0.88	0.98244 (8790)	2577	-	10767	-	-
SDHD	0.90	-	-	-	-	-	-
SDHB	0.92	-	-	-	-	-	-

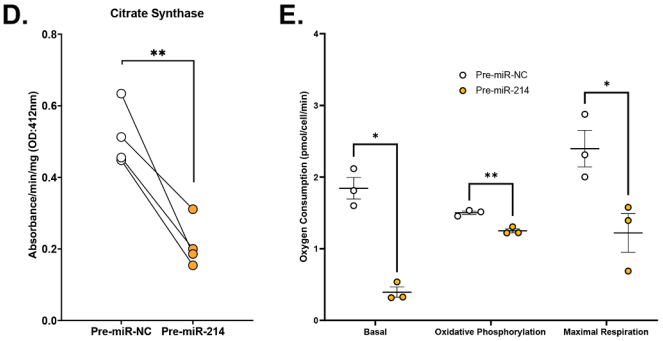

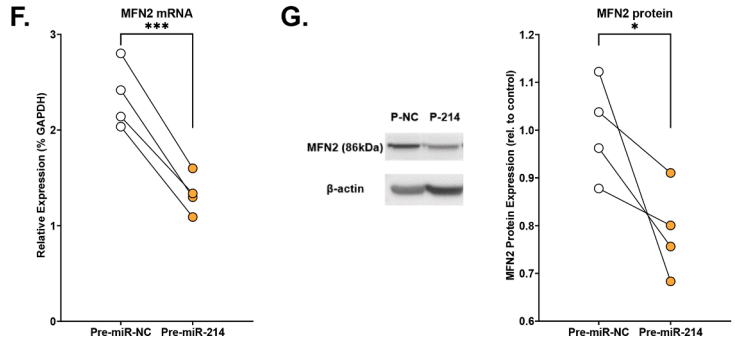

Fig. 7. Mitochondrial protein networks and mitochondrial function are reduced by miR-214–3p in human cardiac fibroblasts. (A) Heat map depicting the most regulated canonical pathways identified by IPA analysis of the TMT proteomics dataset of all altered proteins (increase or decrease), filtered and ranked by statistical significance (P value -log>15). (B) IPA-generated schematic representation of proteins from the "oxidative phosphorylation" pathway mapped to their location. Green diamonds = proteins decreased in the TMT proteomics screen; Blue diamonds = proteins predicted to be inhibited as a result of protein changes in the TMT screen. (C) Summary of pre-miR-214–3p-induced fold-change of some of the component proteins of Complex I (NADH:ubiquinone oxidoreductase; NDUFs) and Complex II (succinate dehydrogenases; SDHs), together with the miR-214–3p:mRNA targeting prediction scores (and ranks) from various target prediction databases. miRabel scores are based on multiple prediction databases (PITA, miRanda, SVMicrO, TargetScan) and are separate from miRDB. (D) Citrate synthase assay of mitochondrial function measured 72 h after transfection of human CF with pre-miR negative control (NC) or pre-miR-214–3p. Paired data from different donor cell populations are linked. $^{**}P < 0.01$ ($n = 4$). (E) Mitochondrial oxygen consumption rate measured by Seahorse Assay analysis at 72 h after transfection of human CF with pre-miR-NC or pre-miR-214–3p. $^{**}P < 0.01$, $^{*}P < 0.05$ ($n = 3$). (F) MFN2 mRNA expression levels measured 48 h after transfection of human CF with pre-miR negative control (NC) or pre-miR-214–3p. Paired data from different donor cell populations are linked. $^{***}P < 0.001$ ($n = 4$). (G) MFN2 protein expression levels measured by western blotting 72 h after transfection of human CF with pre-miR-NC or pre-miR-214–3p. Paired data from different donor cell populations are linked. Representative blot shown, together with β-actin loading control. $^{*}P < 0.05$ ($n = 4$).

effect on proliferation may be influenced by species and/or developmental maturity. Additionally, both prior studies used different methods for measuring proliferation. Whereas we measured proliferation by the gold standard method of cell counting, Sun and colleagues [12] used a BrdU incorporation assay (detecting DNA synthesis) and Yang and colleagues [11] used a cell counting kit-8 assay (CCK8) (detecting cell viability) and the cell-light Edu DNA cell proliferation kit (also detecting DNA synthesis), and so miR-214–3p could be affecting DNA synthesis without affecting the rate of cell division. Importantly, the CCK8 assay relies on the activity of cellular dehydrogenases to detect live cells and so our observed effect of miR-214–3p on mitochondrial function could confer differences in metabolic rate and mitochondrial number that influence the results of the CCK8 assay.

Cardiac remodelling is an orchestrated process involving crosstalk between several different cell types and with the ECM itself. The responses to specific miRNAs are known to be species- and cell type-specific. Therefore miRNA targets, and the resultant phenotypes, may well differ depending on the cell type they are expressed in [5]. We used CF cultures from 6 different patient donors to investigate the impact of miR-214–3p overexpression on the human CF proteome, in the hope of identifying key regulatory networks that underpin cellular function relevant to man. It was important to characterize the cells through confirmation of expression of a range of fibroblast markers and a lack of cardiomyocyte, smooth muscle cell and endothelial cell markers, providing confidence that any observed changes were specific to the fibroblast population. One of the key markers of CFs, COL1A1, was

decreased by 34 % at the protein level and by 36 % at the mRNA level. Exploration of the miRabel database [25], an aggregate of four important human miRNA prediction algorithms (miRanda, PITA, SVmicrO and TargetScan), revealed that COL1A1 is ranked 10,617 out of 11,913 potential miR-214–3p targets, and no seed sequence for miR-214–3p is present in COL1A 3′UTR, hence it is unlikely to be a direct target of miR-214–3p. One possible mechanism for an indirect reduction could be via miR-214–3p targeting enhancer of zeste homolog 1 (EZH1) and −2 (EZH2) which have been shown to increase the expression of peroxisome proliferator-activated receptor-γ (PPAR-γ), and subsequently inhibit the expression of COL1A1 and COL3A1 in mouse myofibroblasts [26].

Our approach to investigate potential miR-214–3p targets from the TMT proteomics screen was twofold. Firstly, we used a guided approach by investigating a small number of proteins known to be influential in cardiac remodelling. Secondly, we took an unbiased approach and used two different bioinformatics tools to identify relationships between differentially expressed proteins to identify key pathways. Piezo1 is a recently discovered mechanosensitive ion channel that plays an important role in converting mechanical signals into altered cellular function across a broad range of tissues, including the heart and cardiovascular system [27]. Piezo1 is one of several types of mechanosensitive ion channels expressed by CF [28], and we originally characterized its expression, signalling and function in mouse and human CF [17]. In CF, Piezo1 is coupled to p38 MAPK activation and expression and secretion of the pro-fibrotic and pro-hypertrophic cytokine IL-6 [17,18,29]. Our findings suggest that miR-214–3p is decreasing Piezo1 protein expression by directly targeting its mRNA, a hypothesis supported by the discovery that the 3′ UTR of PIEZO1 mRNA contains a consensus binding sequence for miR-214–3p. Further studies using PIEZO1 3′UTR luciferase reporter assays would be important for determining whether PIEZO1 is a direct binding target for miR-214–3p. By reducing the expression of Piezo1, miR-214–3p could play a protective role, resulting in reduced influx of Ca^{2+}, p38 MAPK activation and IL-6 secretion, and ultimately protecting against cardiomyocyte hypertrophy and fibrosis.

Our unbiased approach to investigating the TMT proteomics screen firstly used STRING bioinformatics analysis and found that ECM remodelling, and expression of the LOX family of proteins in particular, was modulated by miR-214–3p overexpression. ECM synthesis is necessary in the early stage of remodelling, yet can become dysregulated and pathological in the late stage [30]. LOX family proteins are upregulated in fibrotic disease and act by oxidizing lysine residues in elastin and collagen, facilitating collagen cross linkages which stabilize the proteins and exacerbate fibrosis [31]. In the present study, the entire family of LOX proteins (LOX and LOXL1–4) was increased in response to miR-214–3p overexpression, and this was also evident at the mRNA level, suggesting that miR-214–3p is inhibiting the translation of a putative shared negative regulator (or several coordinated regulators) of the entire LOX family, although such a regulator has not yet been described to our knowledge. Alternatively, miR-214–3p may be acting via a non-canonical mechanism [32], for example increasing specific gene promoter activity, as has been described for some other miRNAs. For example, miR-320 has been proposed to directly increase transcription of the *CD36* (fatty acid translocase) gene in cardiomyocytes in the context of diabetes-induced lipotoxicity [33]. Interestingly, the increase in miR-214–3p expression observed during the acute inflammatory phase of post-MI remodelling (3 days post-MI) coincides with the known peak of LOX family expression post-MI [34], so it is feasible that elevated miR-214–3p contributes to this increase in LOX family expression. Inhibition of LOX activity after MI improves cardiac function [34], so targeting miR-214–3p may have similar potential. Furthermore, we discovered that chronic activation of Piezo1 by Yoda1 resulted in a decrease in LOX, LOXL1 and LOXL4 mRNA expression, which suggests that the miR-214–3p-mediated increase in LOX family expression could be indirect and downstream from a miR-214–3p/Piezo1 axis. This is converse to previous studies demonstrating that Yoda1 treatment resulted in increased LOX expression [35], and with higher levels of Piezo1 expression being associated with higher levels of LOX in HCC [36], and so future investigations should seek to elucidate more precisely the relationship between Piezo1 and the LOX family of enzymes.

Mitochondrial health and homeostasis is vital for the production of ATP and for cellular respiration, and mitochondrial dysfunction occurs in a range of diseases [37]. This is particularly true in cardiac remodelling where cellular respiration, such as in contracting cardiomyocytes or highly proliferative CF and MyoFb, is increased [38]. Mitochondrial dysfunction has been identified as a feature of multiple types of cardiovascular disease including ischemia-reperfusion injury, hypertension, and heart failure, and one of the principal drivers of this is the production of reactive oxygen species (ROS) which induce damage, necrosis and mutations [39]. One of the proteins identified in the IPA analysis of our proteomics screen was the mitochondrial fusion protein, MFN2. This protein is important for the fusing of mitochondria, generating highly efficient cellular mitochondrial networks. In contrast, a decrease in fusion proteins drives a shift toward mitochondrial fission and the breakup of these mitochondrial networks that ultimately leads to decreased mitochondrial efficiency and ROS release. A similar regulation of MFN2 has been demonstrated to promote apoptosis in ischemic acute kidney injury, where miR-214–3p overexpression decreased MFN2 expression and resulted in mitochondrial dysfunction [40]. Moreover, the 3′UTR of *Mfn2* has been validated as a direct target of miR-214–3p using luciferase reporter assays in an investigation that showed miR-214–3p overexpression decreased MFN2 expression in the fibrotic rat heart and in CF [12]. The same study reported that miR-214–3p overexpression induced rat CF proliferation and collagen synthesis via inhibition of MFN2 and activation of ERK1/2 MAPK signalling, resulting in cardiac fibrosis.

Some limitations of our study should be highlighted. In our investigation, pre-miR-214–3p transfection elevated the expression level of miR-214–3p by >1000-fold so it is important to contextualise these findings compared to the more modest increases that would be observed in vivo in response to endogenous stimuli involved in cardiac remodelling. An excess of miR-214–3p over a short period of time favours optimum suppression of protein targets enabling identification of novel targets in this experimental setting. It is unclear whether more modest increases would induce similar effects. It is important to note, however, that 5 of the 20 most down-regulated proteins that were observed in the proteomics screen are known or predicted targets of miR-214–3p, indicating that this level of overexpression retains specificity. Although not in the heart, it is also worth noting that increases in miR-214–3p levels of more than 1000-fold have been reported in samples derived from in vivo lung metastases in mice [41], suggesting that such high increases may have (patho)physiological relevance in some settings. Another limitation was in the methodology of the STRING bioinformatics analysis. STRING creates networks of proteins based solely on a list of proteins, and does not take account of the scale, direction, or reproducibility of expression changes. Nevertheless, it successfully identified LOX-family proteins as being upregulated by miR-214–3p. Interestingly, the LOX/ECM network was not flagged by IPA, underlining the value of using multiple approaches for functional enrichment analysis. Further investigations should seek to explore the exact mechanisms by which miR-214–3p regulates the levels of Piezo1, LOX family proteins and a range of mitochondrial proteins. Due to the decreases in mRNA levels for Piezo1 and MFN2, and the presence of consensus miR-214–3p binding sequences in their 3′UTRs, it is likely that this mechanism is due to a direct binding of miR-214–3p to the 3′UTRs of these mRNA molecules. The mechanism underlying regulation of LOX family proteins appears more complex, as miR-214–3p overexpression increased LOX/LOXL mRNA and protein levels, suggesting that miR-214–3p mediates degradation of one or more putative repressors of the LOX family, or that miR-214–3p is acting via a non-canonical mechanism to directly promote *LOX* gene transcription. It is also possible that regulation and increase in the LOX family of proteins is

linked to a decrease in the collagen family. One hypothesis is that where LOX proteins facilitate collagen crosslinking, the increase in matrix stiffness could produce a mechanical negative feedback loop where collagen protein expression is decreased. This has been shown previously, where *COL1A1* expression is elevated in human immortalised CFs cultured on soft gels compared to stiff gels, with stiffness sensed by α2β1 integrin (ITGA2) [42], which was increased by miR-214–3p overexpression in our own investigation.

MiR-214–3p has been demonstrated herein as a regulator of proteins that play a significant role in the development of cardiac remodelling and of human CF function. The CF has become a therapeutic target of interest in the treatment of adverse remodelling due to its pivotal and central role that influences not only the ECM of the cardiac interstitium and fibrosis, but also the cardiomyocytes and hypertrophy [43]. Exploiting miRNAs as therapeutic targets, either by increasing their expression to downregulate their target mRNAs, or inhibiting them to increase expression of their target mRNAs, is now being considered in drug discovery [44]. An interesting point regarding targeting miR-214–3p as a therapeutic option is that depending on the time point, miR-214–3p activity could be considered beneficial or detrimental. One example of a related miRNA approach for treating cardiac remodelling involved the delivery of an anti-miR-21 at days 5 and 19 after cardiac injury which resulted in reduced cardiac fibrosis, hypertrophy, dampening of inflammatory response and reduced MAPK activation in a pig model of LAD occlusion [45]. A similar approach could therefore be undertaken with the targeting of miR-214–3p in the late phase so that mitochondrial homeostasis is maintained and cellular respiration in surviving CMs is protected. Conversely, miR-214–3p mimics could present a useful therapeutic modality in the early stages after MI, with Aurora and colleagues [21] demonstrating that miR-214–3p overexpression was protective in the acute phase of remodelling following MI. Similarly, increasing miR-214–3p expression to reduce Piezo1 levels could protect against fibrosis and hypertrophy.

Conclusions

This work has discovered that miR-214–3p is upregulated during cardiac remodelling and that its activity is particularly apparent in the early stages of cardiac remodelling. MiR-214–3p overexpression in human CF resulted in the decrease of Piezo1 mRNA and protein expression, as well as reducing Piezo1-mediated intracellular Ca^{2+} influx in human CF. A bioinformatics-based approach found that miR-214–3p increases the family of LOX proteins at the mRNA and protein level, indicating important roles in ECM turnover and fibrosis. Finally, miR-214–3p overexpression resulted in a decrease in mitochondrial activity and density, likely due to reduced MFN2 mRNA levels. All of these roles indicate miR-214–3p as an important regulator that should be further investigated for its role in cardiac remodelling in vivo.

Experimental procedures

Human cardiac fibroblast culture

Biopsies of human right atrial appendage were obtained from non-diabetic patients without left ventricular dysfunction undergoing elective coronary artery bypass grafting at the Leeds General Infirmary, following local ethical committee approval and informed patient consent (study references 01/040 and 17/WA/0314). Summary data for the total cohort of patient donors used for generating cells is $n = 38$, 85 % male, mean age = 68.0 ± 0.9. The study accords with the Declaration of Helsinki principles. Cultures of CF were established using a collagenase digestion and differential plating method as described previously [46]. Cells were cultured under sterile conditions in full growth medium (FGM) comprising Dulbecco's modified Eagle medium supplemented with 10 % FCS (Biosera), 1 % l-Glutamine and 1 % penicillin / streptomycin / Amphotericin B (Gibco) in a humidified atmosphere of 5 % CO_2 in air at 37 °C, and subsequently passaged by trypsinisation (using Trypsin-EDTA 0.25 %). Early passage cells (P1) were frozen in liquid nitrogen in 10 % DMSO in FCS for future use. Experiments were performed after serum-starving in serum-free medium (SFM) for 24 h, and treatments were performed in SFM. Cells were used at early passage (P2–5) and all experiments used cells from different donors for each biological replicate.

Mouse cardiac fibroblast culture

C57BL/6 J mice (10–14 weeks old) were humanely euthanized by cervical dislocation in accordance with the Animal Scientific Procedures Act of 1986 under UK Home Office authorization. Murine CFs were harvested from whole hearts by collagenase digestion and cultured as described previously [10]. Murine CFs were used at early passage (P1–2).

RNA isolation

RNA for both miRNA RT-PCR and mRNA RT-PCR was isolated from human and murine CF using the Aurum Total RNA Mini Kit (Bio-Rad), a spin-based RNA elution method, as per the manufacturer's instructions. This kit produced 80 μL of DNA-free, total RNA which was stored at −80 °C. RNA samples from murine heart cells were prepared from cell fractions obtained by magnetic antibody cell separation (MACS; Miltenyi Biotec), as previously described [10]. Specific RNA samples from remodelling mouse heart were obtained using the TRIzol technique during our previous studies involving ISO infusion [10] and LAD ligation [47]. For ISO infusion, Alzet 1002 mini-osmotic pumps were implanted subcutaneously in isoflurane-anesthetized male mice at 10–12 weeks of age and saline or ISO (30 mg/kg/d) was infused for 14 days. Pumps were then removed under anaesthesia, mice allowed to recover, and hearts collected 7 days later [10]. The permanent LAD coronary artery ligation model of experimental MI was performed on isoflurane-anesthetized male mice at 10–12 weeks of age and involved ligation of the LAD at the edge of the left atrium using prolene sutures [47]. RNA was extracted at 3 days post-LAD ligation from Cre-negative controls from a cardiomyocyte-specific IL-1α knock out (KO) (MIL1AKO) mouse line [47]. Mice from which RNA was extracted at 4 weeks post-MI were Cre-negative controls for a fibroblast-specific IL-1R1 KO (FIL1R1KO) mouse line that had been injected with tamoxifen for 5 days, at 12 days old before performing LAD ligation at 10–12 weeks of age [47].

miRNA real-time RT-PCR

cDNA was synthesized using the TaqMan MicroRNA Reverse Transcription Kit and TaqMan MicroRNA Assay (miR-214–3p #002306; miR-21a #000397; miR-224 #000599; or miR-30d #000420), as well as U6 snRNA (#001973) as a housekeeping control, as per manufacturer's instructions (ThermoFisher). cDNA samples were immediately processed for RT-PCR analysis using 96-well plates and the QuantStudio 3 Real Time PCR System (ThermoFisher). For miRNA RT-PCR, a mastermix of 18 μL per well was prepared containing 7.25 μL nuclease free water, 10 μL TaqMan Universal Master Mix II (no UNG) and 0.75 μL specific TaqMan MicroRNA Assay RT primers (depending on the miRNA of interest, or U6 snRNA as a housekeeping control) per sample. To each of these wells, 2 μL of miRNA cDNA was dispensed. Data were analysed using the $2^{-\Delta CT}$ method.

Gene expression real-time RT-PCR

cDNA synthesis was performed using the Reverse Transcription System (Promega), according to the manufacturer's protocol. For real-time RT-PCR in 96-well plates, a mastermix of 18 μL per well was prepared containing 7.5 μL of nuclease free water, 10 μL of TaqMan Gene Expression Master Mix and 0.5 μL of specific TaqMan Real-Time PCR Assay primers (COL1A1 Hs00164004_m1; LOX Hs00942483_m1; LOXL1 Hs00935937_m1; LOXL2 Hs00158757_m1; LOXL3 Hs01046941_g1; LOXL4 Hs00260059_m1; MFN2 Hs00208382_m1; PIEZO1 Hs00207230_m1 or GAPDH Hs99999905_m1 as a housekeeping

control). 18 μL of mastermix was then aliquoted into each well of a 96 well plate and 2 μL of cDNA added. PCR was performed using the QuantStudio 3 Real Time PCR System (ThermoFisher) and data analysed using the $2^{-\Delta CT}$ method.

Transfection of cultured human cardiac fibroblasts

Human CF were seeded at a density of 70,000 cells/well into a 6-well plate in 2 mL FGM and incubated for 24 h at 37°C. Transfection reagents (Lipofectamine 2000, OptiMEM) were prepared according to manufacturer's instructions (ThermoFisher). Pre-miR™ miRNA Precursors (hsa-pre-miR-214–3p PM12124; pre-miR negative control (NC) AM17110) were purchased from ThermoFisher and transfected at a final concentration of 30 nM for 6 h. Medium was changed to FGM following transfection to allow cell recovery. Note that these commercially available pre-miRs are small, chemically modified double-stranded RNA molecules designed to mimic endogenous mature miRNAs. They are not hairpin constructs and should not be confused with pre-miRNAs.

Cell proliferation

Human CF proliferation assays were performed as described previously [46]. Briefly, pre-miR-transfected cells from four different donors were seeded at a density of 10,000 cells/well in a 24-well plate in 1 mL FGM and incubated for 24 h at 37°C before serum-starving for a further 48 h. Medium (SFM or 2.5 % FCS-containing DMEM) was replaced every 2 days throughout the experiment and cell number was determined in triplicate wells after 7 days by trypsinising and counting viable cells using Trypan Blue and a haemocytometer. Triplicate counts were averaged to determine a mean cell count for each biological replicate.

TMT proteomics

Cellular protein expression was measured by tandem mass tagging (TMT) in protein lysates isolated from human CF from six donors (all male, non-diabetic, mean age = 64.2 ± 2.4), 72 h after pre-miR-negative control (NC) or pre-miR-214–3p transfection. Protein lysates were obtained by scraping cells from three wells of a 6-well plate into 1X RIPA lysis buffer (containing 1 % PPI cocktail II and 1 % PPI cocktail III; Merck). After sonication for 30 s at 4 °C, the mixture was centrifuged at 14,000 x g for 15 min and the supernatant subsequently stored at −80 °C. Protein samples (>100 μg/mL) underwent TMT analysis as a service provided by the University of Bristol Proteomics Facility. Samples (50 μg) were digested and labelled using TMT reagents (amine-specific isobaric tags). Reverse phase (RP) chromatography was performed to fractionate the samples and then each fraction was analysed by acidic RP nano-LC MS/MS using the SPS-MS3 approach on an Orbitrap Fusion Lumos mass spectrometer. Two 10-plex experiments were performed each containing 9 samples plus a common pooled reference sample (which contained an aliquot of every sample, acting as an internal reference) whereby tagged peptides were used to track protein expression.

The raw data files were processed and quantified using Proteome Discoverer software v2.1 (Thermo Scientific) and searched against the UniProt Human database (downloaded January 2022: 178,486 entries) using the SEQUEST HT algorithm. Peptide precursor mass tolerance was set at 10 ppm, and MS/MS tolerance was set at 0.6 Da. Search criteria included oxidation of methionine (+15.995 Da), acetylation of the protein N-terminus (+42.011 Da) and methionine loss plus acetylation of the protein N-terminus (−89.03 Da) as variable modifications and carbamidomethylation of cysteine (+57.021 Da) and the addition of the TMT mass tag (+229.163 Da) to peptide N-termini and lysine as fixed modifications. Searches were performed with full tryptic digestion and a maximum of 2 missed cleavages were allowed. The reverse database search option was enabled, and all data were filtered to satisfy FDR of 5 %.

This analysis was used to generate an Excel report listing the proteins identified, abundances, generation of volcano plots and principal component analysis. In total, 8793 proteins were identified. Non-human proteins, contaminants and proteins that fell below the FDR cut-off of 5 % were subsequently eliminated from the downstream bioinformatics analysis. The remaining proteins were filtered based on the most significantly changed proteins (by P value) and the largest fold changes (either decreased or increased) based on the log2 fold change results from the original analysis.

Network analysis

Bioinformatics analyses were performed on the filtered dataset using two tools; Search Tool for the Retrieval of Interacting Genes/Proteins (STRING) [48] and Ingenuity Pathway Analysis (IPA) [49]. The free-to-use bioinformatics tool STRING makes predictions on shared networks between the proteins in the dataset. Statistically significantly altered proteins were ranked in three different ways: (i) by P value, (ii) by fold decrease and (iii) by fold increase. STRING analysis was then performed on the top 50 proteins from each list. Individual proteins that did not form networks were removed from the STRING analysis figures for clarity.

IPA (Qiagen, Germany) was used to predict canonical pathways, upstream regulators, and diseases and functions in which the proteins altered by miR-214–3p overexpression were likely to be involved. Each of the canonical pathways were investigated based on the significance value of the pathway (which indicated the strength of the prediction), the specific targets from the protein list that were implicated in the pathway (including direction of change), and the location of each of these proteins in the pathway based on a graphical description generated within IPA.

Flex station measurement of Piezo1 activity

Intracellular Ca^{2+} measurements were taken using a 96-well fluorescence plate reader (FlexStationII 384, Molecular Devices) and the ratiometric Ca^{2+} indicator dye Fura2-AM, as described previously [17]. Human CF were plated 48 h after pre-miR transfection at a density of 12,000 cells/well in FGM in a 96-well poly-d-lysine coated, black wall/clear bottom plate and incubated overnight at 37 °C. Fura2-AM was added to the cells for 30 min in standard bath solution (SBS) containing pluronic acid and probenecid [17]. After washing in SBS, stimuli (5 μM Yoda1; DMSO vehicle) were introduced after 60 s and readings taken for a total run time of 7 min at intervals of 5 s. ATP (5 μM) was added after 300 s. The change in intracellular Ca^{2+} concentration ($\Delta[Ca^{2+}]_i$) was measured as the ratio of Fura-2 emission (510 nm) intensity at 340 nm and 380 nm.

Citrate synthase assay

Mitochondrial function was assessed using a citrate synthase (CS) assay, as described previously [20,50]. The assay was performed in a 96-well plate at 37 °C using 100 mM Tris–HCl, 0.2 mM acetyl CoA, 0.1 mM 5,5′-dithiobis 2-nitrobenzoic acid (DTNB) and 1 mM oxaloacetate, pH 8.0. Experimental wells contain 199 μL of working solution plus 1 μL of protein lysate sample or CS standard (all in triplicate). CS activity was measured at 412 nm for 5 min using a 96-well spectrophotometer (PowerWave, Biotek). Absorbance was calculated based on the amount of protein in each sample, measured using a BCA assay. Data were expressed as A_{412} per min per mg cell lysate.

Seahorse assay

Mitochondrial metabolic activity was measured using the Seahorse XF-96 Extracellular Flux Analyzer (Seahorse Biosciences, North Billeric, MA, USA) to measure oxygen concentration rate (OCR) on attached

human CF. This protocol has been described previously [51]. Briefly, fibroblasts were plated in XF 96-well Seahorse plates (V3-PS; 101, 085–004). Prior to analysis, the culture medium was replaced with unbuffered XF assay medium containing sodium pyruvate, l-glutamine and glucose at pH 7.4 and cells were then allowed to equilibrate in a humid non-CO_2 incubator immediately before metabolic flux analysis. OCR was measured under both basal conditions and after injection of oligomycin, FCCP and Rotenone/Antimycin A. Hoechst staining was used to standardise to cell number [52]. In brief, cells were fixed in 70 % ethanol and left to dry. DNA-binding fluorochrome Hoechst 33,258 was added to the wells for 5 min and then cells were washed with distilled water. Once dry, the fluorescence of each well was measured (Hoechst 350 nm excitation and 450 nm emission wavelengths) to determine the relative cell number in each well.

Statistical analyses

GraphPad Prism 8 (San Diego, CA, USA) was used for data analysis and presentation. Data are depicted as scatterplots (paired data are linked by a line), and "n" represents the number of independent experiments on cells from different donors (i.e. biological replicates). For comparisons between two sets of normalized data (e.g. RT-PCR), values were firstly log transformed to facilitate assessment of fold changes. Unpaired *t* tests were performed to calculate a two-tailed P value when comparing data deriving from different biological samples and paired *t* tests performed for data belonging to cells from the same patients. A two-way ANOVA was performed to measure significance across two different variables, followed by a Tukey post-hoc test. $P < 0.05$ was considered statistically significant.

Declaration of generative AI and AI-assisted technologies in the writing process

The authors did not use generative AI or AI-assisted technologies in the writing of this manuscript.

Supplementary Information

The mass spectrometry proteomics data have been deposited to the ProteomeXchange Consortium via the PRIDE [53] partner repository with the dataset identifier PXD045875.

Data availability

The mass spectrometry proteomics data have been deposited to the ProteomeXchange Consortium via the PRIDE partner repository with the dataset identifier PXD045875.

Acknowledgements

We are grateful to the many patient donors for allowing use of their tissue for culturing cells, and to the cardiothoracic surgeons at Leeds Teaching Hospitals (Mr David O'Regan and Mr Sotiris Papaspyros) for provision of atrial appendage biopsies. We thank the University of Bristol Proteomics Facility for performing the TMT proteomics and preliminary data analysis. Biorender licensed software was used to generate Fig. 3A (Biorender.com).

Funding

This work was supported by a British Heart Foundation PhD Studentship (FS/19/41/34478) awarded to N. A. T., K. A. F. and C. J. T. (student).

Supplementary materials

Supplementary material associated with this article can be found, in the online version, at doi:10.1016/j.matbio.2024.06.005.

References

[1] K.E. Porter, N.A. Turner, Cardiac fibroblasts: at the heart of myocardial remodeling, Pharmacol. Ther. 123 (2) (2009) 255–278.
[2] F. Klingberg, B. Hinz, E.S. White, The myofibroblast matrix: implications for tissue repair and fibrosis, J. Pathol. 229 (2) (2013) 298–309.
[3] N.A. Turner, K.E. Porter, Function and fate of myofibroblasts after myocardial infarction, Fibrogenesis. Tissue Repair. 6 (1) (2013) 5.
[4] B. Sedgwick, et al., Investigating inherent functional differences between human cardiac fibroblasts cultured from nondiabetic and Type 2 diabetic donors, Cardiovasc. Pathol. 23 (4) (2014) 204–210.
[5] J. O'Brien, et al., Overview of MicroRNA biogenesis, mechanisms of actions, and circulation, Front. Endocrinol. (Lausanne) 9 (2018) 402.
[6] C.J. Stavast, S.J. Erkeland, The non-canonical aspects of microrna: many roads to gene regulation, Cells 8 (11) (2019).
[7] H.C. Stevens, et al., Regulation and function of miR-214 in pulmonary arterial hypertension, Pulm. Circ. 6 (1) (2016) 109–117.
[8] B. Dai, et al., The cell type-specific functions of miR-21 in Cardiovascular Diseases, Front. Genet. 11 (2020) 563166.
[9] X.l. Zhou, et al., miR-21 promotes cardiac fibroblast-to-myofibroblast transformation and myocardial fibrosis by targeting Jagged1, J. Cell. Mol. Med. 22 (8) (2018) 3816–3824.
[10] S.A. Bageghni, et al., Cardiac fibroblast-specific p38α MAP kinase promotes cardiac hypertrophy via a putative paracrine interleukin-6 signaling mechanism, The FASEB Journal 32 (9) (2018) 4941–4954.
[11] K. Yang, et al., The deficiency of miR-214-3p exacerbates cardiac fibrosis via miR-214-3p/NLRC5 axis, Clin. Sci. (Lond.) 133 (17) (2019) 1845–1856.
[12] M. Sun, et al., MicroRNA-214 mediates isoproterenol-induced proliferation and collagen synthesis in cardiac fibroblasts, Sci Rep 5 (1) (2015) 18351.
[13] M.M.J. Amin, C.J. Trevelyan, N.A. Turner, MicroRNA-214 in Health and Disease, Cells 10 (12) (2021).
[14] H. Xia, L.L. Ooi, K.M. Hui, MiR-214 targets β-catenin pathway to suppress invasion, stem-like traits and recurrence of human hepatocellular carcinoma, PLoS ONE 7 (9) (2012) e44206.
[15] J. Liu, et al., miR-214 targets the PTEN-mediated PI3K/Akt signaling pathway and regulates cell proliferation and apoptosis in ovarian cancer, Oncol. Lett. 14 (5) (2017) 5711–5718.
[16] M.J. Ivey, M.D. Tallquist, Defining the cardiac fibroblast, Circ. J. 80 (11) (2016) 2269–2276.
[17] N.M. Blythe, et al., Mechanically activated Piezo1 channels of cardiac fibroblasts stimulate p38 mitogen-activated protein kinase activity and interleukin-6 secretion, J. Biol. Chem. 294 (46) (2019) 17395–17408.
[18] F. Bartoli, et al., Global PIEZO1 gain-of-function mutation causes cardiac hypertrophy and fibrosis in mice, Cells 11 (7) (2022).
[19] R. Syeda, et al., Chemical activation of the mechanotransduction channel Piezo1, Elife 4 (2015) e07369.
[20] A. Whitehead, et al., Brown and beige adipose tissue regulate systemic metabolism through a metabolite interorgan signaling axis, Nat Commun 12 (1) (2021) 1905.
[21] A.B. Aurora, et al., MicroRNA-214 protects the mouse heart from ischemic injury by controlling Ca^{2+} overload and cell death, J. Clin. Invest. 122 (4) (2012) 1222–1232.
[22] Y.Q. Ding, et al., MicroRNA-214 contributes to Ang II-induced cardiac hypertrophy by targeting SIRT3 to provoke mitochondrial malfunction, Acta Pharmacol. Sin. 42 (9) (2021) 1422–1436.
[23] S.A. Leancă, et al., Left Ventricular Remodeling after Myocardial Infarction: from Physiopathology to Treatment, Life (Basel) 12 (8) (2022).
[24] F. Bouzegrhane, G. Thibault, Is angiotensin II a proliferative factor of cardiac fibroblasts? Cardiovasc. Res. 53 (2) (2002) 304–312.
[25] A. Quillet, et al., Improving bioinformatics prediction of microrna targets by ranks aggregation, Front. Genet. 10 (2019) 1330.
[26] W.S. Zhu, et al., Targeting EZH1 and EZH2 contributes to the suppression of fibrosis-associated genes by miR-214-3p in cardiac myofibroblasts, Oncotarget 7 (48) (2016) 78331–78342.
[27] D.J. Beech, A.C. Kalli, Force sensing by piezo channels in cardiovascular health and disease, Arterioscler. Thromb. Vasc. Biol. 39 (11) (2019) 2228–2239.
[28] L. Stewart, N.A. Turner, Channelling the force to reprogram the matrix: mechanosensitive ion channels in cardiac fibroblasts, Cells 10 (5) (2021).
[29] R. Emig, et al., Piezo1 channels contribute to the regulation of human atrial fibroblast mechanical properties and matrix stiffness sensing, Cells 10 (3) (2021).
[30] C. Bonnans, J. Chou, Z. Werb, Remodelling the extracellular matrix in development and disease, Nat. Rev. Mol. Cell Biol. 15 (12) (2014) 786–801.
[31] S. Kumari, T.K. Panda, T. Pradhan, Lysyl oxidase: its diversity in health and diseases, Indian J. Clin. Biochem. 32 (2) (2017) 134–141.
[32] D. Santovito, C. Weber, Non-canonical features of microRNAs: paradigms emerging from cardiovascular disease, Nat. Rev. Cardiol. 19 (9) (2022) 620–638.
[33] H. Li, et al., Nuclear miR-320 Mediates Diabetes-Induced Cardiac Dysfunction by Activating Transcription of Fatty Acid Metabolic Genes to Cause Lipotoxicity in the Heart, Circ. Res. 125 (12) (2019) 1106–1120.
[34] J. González-Santamaría, et al., Matrix cross-linking lysyl oxidases are induced in response to myocardial infarction and promote cardiac dysfunction, Cardiovasc. Res. 109 (1) (2015) 67–78.
[35] Y. Doki, et al., Piezo1 channel causes lens sclerosis via transglutaminase 2 activation, Exp. Eye Res. 237 (2023) 109719.
[36] M. Li, et al., Activation of Piezo1 contributes to matrix stiffness-induced angiogenesis in hepatocellular carcinoma, Cancer Commun. (Lond) 42 (11) (2022) 1162–1184.

[37] G.L. Nicolson, Mitochondrial Dysfunction and Chronic Disease: treatment With Natural Supplements, Integr. Med. (Encinitas) 13 (4) (2014) 35–43.
[38] G. Siasos, et al., Mitochondria and cardiovascular diseases-from pathophysiology to treatment, Ann. Transl. Med. 6 (12) (2018) 256.
[39] A.V. Poznyak, et al., The role of mitochondria in cardiovascular diseases, Biology. (Basel) 9 (6) (2020).
[40] Y. Yan, et al., miR-214 represses mitofusin-2 to promote renal tubular apoptosis in ischemic acute kidney injury, Am. J. Physiol. Renal. Physiol. 318 (4) (2020) F878–f887.
[41] E. Penna, et al., microRNA-214 contributes to melanoma tumour progression through suppression of TFAP2C, EMBO J. 30 (10) (2011) 1990–2007.
[42] M. Gałdyszyńska, et al., The stiffness of cardiac fibroblast substrates exerts a regulatory influence on collagen metabolism via α2β1 Integrin, FAK and Src kinases, Cells 10 (12) (2021).
[43] R.D. Brown, et al., The cardiac fibroblast: therapeutic target in myocardial remodeling and failure, Annu. Rev. Pharmacol. Toxicol. 45 (2005) 657–687.
[44] B. Laggerbauer, S. Engelhardt, MicroRNAs as therapeutic targets in cardiovascular disease, J. Clin. Invest. 132 (11) (2022).
[45] R. Hinkel, et al., AntimiR-21 Prevents Myocardial Dysfunction in a Pig Model of Ischemia/Reperfusion Injury, J. Am. Coll. Cardiol. 75 (15) (2020) 1788–1800.
[46] N.A. Turner, et al., Chronic beta2-adrenergic receptor stimulation increases proliferation of human cardiac fibroblasts via an autocrine mechanism, Cardiovasc. Res. 57 (3) (2003) 784–792.
[47] S.A. Bageghni, et al., Fibroblast-specific deletion of interleukin-1 receptor-1 reduces adverse cardiac remodeling following myocardial infarction, JCI. Insight. 5 (17) (2019).
[48] D. Szklarczyk, et al., The STRING database in 2023: protein-protein association networks and functional enrichment analyses for any sequenced genome of interest, Nucleic. Acids. Res. 51 (D1) (2023) D638–d646.
[49] A. Krämer, et al., Causal analysis approaches in ingenuity pathway analysis, Bioinformatics. 30 (4) (2014) 523–530.
[50] P. Houle-Leroy, et al., Effects of voluntary activity and genetic selection on muscle metabolic capacities in house mice Mus domesticus, J. Appl. Physiol. (1985) 89 (4) (2000) 1608–1616.
[51] L. Zdrazilova, H. Hansikova, E. Gnaiger, Comparable respiratory activity in attached and suspended human fibroblasts, PLoS ONE 17 (3) (2022) e0264496.
[52] J. Bucevičius, G. Lukinavičius, R. Gerasimaitė, The use of hoechst dyes for DNA staining and beyond, Chemosensors 6 (2) (2018) 18.
[53] Y. Perez-Riverol, et al., The PRIDE database resources in 2022: a hub for mass spectrometry-based proteomics evidences, Nucleic. Acids. Res. 50 (D1) (2022) D543–d552.